ligands are coordinated in the plane of the cluster core. The cdo ligands of **2a** interact via two O–H–O hydrogen bonds (O···O = 2.47(2) and 2.51(2) Å), shown in dotted lines. The out-of-plane coordination sites are occupied by four acetate ligands. Two act as bridging ligands between Pt(1) and Pt(2) and between Pt(2) and Pt(3), and the remaining two are coordinated in a unidentate fashion to Pt(1) and Pt(3). No direct bridge exists between Pt(1) and Pt(3) (long Pt–Pt bond), but the two O(cdo)–H–O(CH_3COO) hydrogen-bonded bridges are shown in dashed lines. If the Pt–Pt bond is included, the coordination geometry around each Pt is a distorted octahedron. The ^1H-, ^{13}C-, and ^{195}Pt-NMR spectra[8] of **2a** show that the solid-state structure is retained in a solution state.

On the other hand, the reaction of **1** with $dmgH_2$ gave two kinds of red-brown crystalline solids in the same procedure, $[Pt_3(CH_3COO)_4(dmgH)_2(dmgH_2)]$ (**2b**)[12] and $[Pt_4(CH_3COO)_5(dmgH)_3]$ (**3b**).[13] Yields of **2b** and **3b** were approximately 5 and 75%, respectively, under our experimental conditions. The ^1H-, ^{13}C-, and ^{195}Pt-NMR spectra of compound **2b**[12] allow unambigous assignment of a triangular cluster structure very similar to **2a**.

The preliminary X-ray structure of **3b**[14] is shown schematically in Chart I. This compound is tetranuclear and consists of two units, a triangular cluster core very similar to that in **2b** and a mononuclear unit with square planar geometry. There are no Pt–Pt bonds between the units, and the in-plane coordination sites of the triangular core are all occupied by the dmg ligands. The structure shows the partial removal of one Pt from the tetranuclear cluster core of **1**. When one Pt atom in the mononuclear unit and the unidentate acetate attached to the Pt atom are removed from the structure **3b**, a residual structure is essentially the same as **2b**. Disposition of the four out-of-plane acetates in **1** remains almost unchanged in **3b**. In actual fact, **3b** converts to **2b** in acetone solution in the presence of an excess of free $dmgH_2$ ligand in a 4–5% yield under conditions similar to those in the reactions between **1** and the oximes. These facts may suggest that **2b** is formed via **3b**, although details are not certain at this moment. In the case of the $cdoH_2$ reaction, a tetranuclear compound corresponding to **3b** was detected as only a very weak chromatographic band. The transformation mechanism is now being studied.

When **1** is allowed to react with $cdoH_2$ or $dmgH_2$, in-plane ligand substitution takes place initially, as evidenced by the fact that the in-plane coordination sites in **2a**, **2b**, and **3b** are all occupied by the oxime ligands. The incoming oxime ligands take up a chelate coordination mode rather than the bridge coordination of acetates in **1**. Because of the steric demands of the bulky oxime ligands at the in-plane sites, one Pt in the square planar cluster of **1** is pushed out from the core to yield the triangular cluster. The oxidation state of Pt atoms in the products **2a**, **2b**, and **3b** remains in the +2 state. To our knowledge, the present complexes are the first compounds with triangular Pt(II) cluster cores, although similar triangular cluster cores are known for low-valent Pt.[1,2]

Acknowledgment. This work was supported by Grants-in-Aid for Scientific Research (Nos. 02303006 and 04241102) from the Ministry of Education, Science, and Culture, Japan.

Supplementary Material Available: Tables of crystallographic data, experimental conditions, atomic positional and thermal parameters, and interatomic distances and bond angles for **2a**·$2CH_3CN$ (10 pages); tables of observed and calculated structure factors (43 pages). Ordering information is given on any current masthead page.

---

[10] EHMO calculation for the triangular model compound $[Pt_3(HCOO)_4(glyH)_2(glyH_2)]$ ($glyH_2$ = glyoxime) showed clearly the presence of three Pt–Pt single bonds between neighboring Pt atoms in the triangle. The calculation was carried out in a way similar to that reported previously for **1**.[7]

[11] Palladium(II) acetate, $Pd_3(CH_3COO)_6$, also has triangular structure, although it has no direct Pd–Pd bond (Skapski, A. C.; Smart, M. L. *J. Chem. Soc., Chem. Commun.* **1970**, 658).

[12] Anal. Calcd for $Pt_3O_{14}N_6C_{20}H_{34}$: C, 20.57; H, 2.94; N, 7.20. Found: C, 21.47; H, 3.13; N, 6.93. FABMS: 1168 (calcd MW = 1167.6). NMR data (JEOL JNM-GSX-270 FT NMR spectrometer) in $CDCl_3$: ^1H, δ 1.79, 1.85 (s, 6 H, acetate-CH_3), 2.35, 2.40, 2.40 (s, 6 H, dmg-CH_3), 12.22 (s, 2 H, NOH, which are not involved in the hydrogen bond); ^{13}C, δ 12.77, 12.94, 13.16 (dmg-CH_3), 21.25, 21.62 (acetate-CH_3), 149.31, 150.33, 155.59 (N=C), 179.58, 192.07 (COO); ^{195}Pt, δ 1035.1 (2 Pt), 1038.7 (1 Pt) (vs K_2PtCl_4 in D_2O).

[13] Anal. Calcd for $Pt_4O_{16}N_6C_{22}H_{36}$: C, 18.61; H, 2.49; N, 5.92. Found: C, 18.67; H, 2.55; N, 5.54. FABMS: 1420 (calcd MW = 1421.0).

[14] Crystal data: $Pt_4(CH_3COO)_5(dmgH)_3 = Pt_4O_{16}N_6C_{22}H_{36}$, triclinic, space group $P\bar{1}$, $a = 12.106(3)$, $b = 16.229(2)$, and $c = 11.752(2)$ Å, $\alpha = 95.39(1)$, $\beta = 115.37(1)$, $\gamma = 97.81(2)°$, $V = 2036.8(7)$ Å^3, $Z = 2$, current $R = 7.8\%$. A unidentate acetate attached to the Pt atom in the mononuclear unit is disordered except for the donor oxygen.

Solution EPR Spectra of Reactive 1,5- and 1,6-Biradicals

Malcolm D. E. Forbes

Department of Chemistry, Venable and Kenan Laboratories
University of North Carolina
Chapel Hill, North Carolina 27599-3290

Received December 3, 1992

Biradicals of six carbon atoms chain length and shorter are often postulated as reactive intermediates in organic reaction mechanisms.[1] The structural and electronic properties of such species have long been difficult to quantify, with transient optical spectroscopy and product analyses being the predominant characterization tools.[2] The recent advance of time-resolved magnetic resonance techniques[3] in the study of biradicals has, to date, been applicable only to longer chains (1,7- and longer) where the singlet–triplet splitting ($2J$) is small enough to allow substantial mixing of the EPR active triplet sublevels with the highly reactive singlet level.[4] As the biradicals become shorter, large J values lead to a small degree of singlet–triplet mixing, which in turn leads to weak polarization of the EPR active populations. This situation is depicted graphically in Figure 1. The resulting EPR signals are then below the sensitivity limit of a typical X-band (9.5 GHz) spectrometer operating without field modulation.[5] Two strategies exist for overcoming this problem. The first is to alter the structure of the biradical so that the value of $|2J|$ is decreased, moving the singlet state closer to at least one of the triplet levels (usually T^-, the lowest level). This can be accomplished by restricting the number of conformations with large overlap between the unpaired electrons or by delocalization of the electrons into aromatic rings. The second strategy is to move the time-resolved EPR experiment (TREPR) to a higher frequency (Q-band, 35 GHz), pushing the T^- level closer to the singlet via a larger Zeeman interaction. In this communication we report the successful combination of both strategies to obtain the solution EPR spectra of 1,5- and 1,6-bis(benzyl) biradicals, using the photochemistry shown in Scheme I. These are the first solution EPR spectra of transient biradicals with a chain length of less than seven carbon atoms at either frequency.[6]

---

[1] *Kinetics and Spectroscopy of Carbenes and Biradicals*; Platz, M., Ed.; Plenum: New York, 1990.

[2] (a) Johnston, L. J.; Scaiano, J. C. *Chem. Rev.* **1989**, *89*, 521. (b) Lei, X. L.; Doubleday, C. E., Jr.; Zimmt, M. B.; Turro, N. J. *J. Am. Chem. Soc.* **1986**, *108*, 2444.

[3] (a) Trifunac, A. D.; Lawler, R. G.; Bartels, D. M.; Thurnauer, M. C. *Prog. React. Kinet.* **1986**, *14*, 43. (b) Closs, G. L.; Redwine, O. D. *J. Am. Chem. Soc.* **1985**, *107*, 4543. (c) Closs, G. L.; Redwine, O. D. *J. Am. Chem. Soc.* **1985**, *107*, 6131. (d) Closs, G. L.; Forbes, M. D. E. *J. Am. Chem. Soc.* **1987**, *109*, 6185.

[4] (a) Closs, G. L.; Forbes, M. D. E.; Piotrowiak, P. *J. Am. Chem. Soc.* **1992**, *114*, 3285. (b) Closs, G. L.; Forbes, M. D. E. *J. Phys. Chem.* **1991**, *95*, 1924.

[5] The minimum detectable number of spins in direct detection experiments is usually at least 1 order of magnitude greater than that in field-modulated experiments, i.e., approximately 10^{13} per sample for our X-band spectrometer.

0002-7863/93/1515-1613$04.00/0

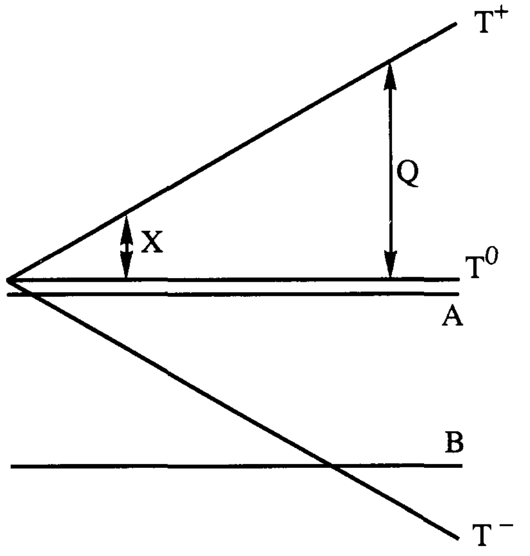

Figure 1. Energy level diagram showing biradical energy levels T^+, T^0, and T^- as a function of applied magnetic field $\mathbf{B}_0$. Energy level A indicates the singlet level for a long-chain biradical with a small J coupling, while B is for a short-chain biradical with a large (negative) J. The singlet–triplet energy gap ($-2J$) is the energy difference between S and T^0. Microwave quanta for X-band and Q-band are shown as bold double arrows.

Scheme I

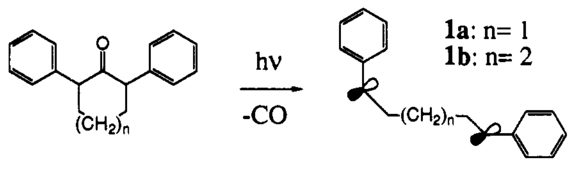

1

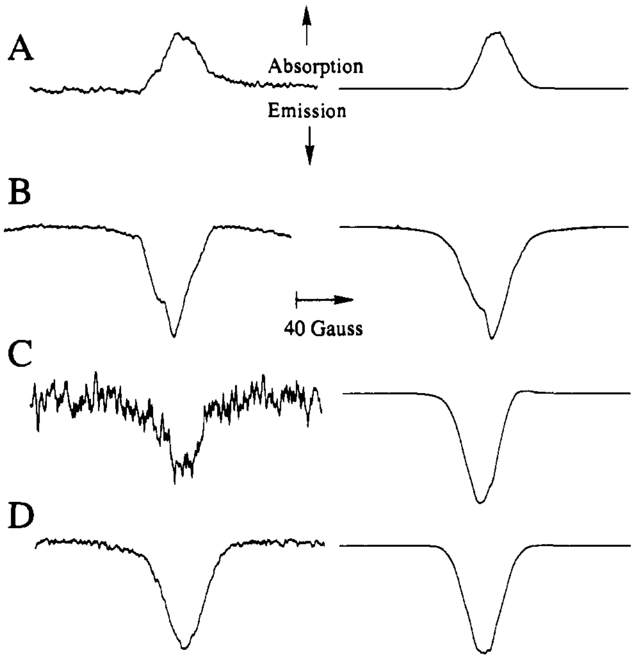

Figure 2. Experimental (left) and simulated (right) time-resolved EPR spectra of biradicals **1a** and **1b** taken in N_2-saturated benzene solution of the precursors[14] (0.04–0.08 M) at 25 °C. The X-band and Q-band spectra are centered at 3380 and 12540 G, respectively. (A) X-band spectrum of **1b** taken with the boxcar gate opening 0.5 μs after the laser flash. (B) Q-band spectrum of **1b** at 0.5 μs. (C) X-band spectrum of biradical **1a** taken at 100 ns. (D) Q-band spectrum of **1a** at 200 ns. In the simulations, literature values for the g-factors of the corresponding monoradicals[15] were found to be satisfactory, and hyperfine coupling constants were taken from studies of monoradicals of similar structure.[16] Parameters common to all four spectra are as follows: hyperfine coupling constants: $2a_H$(benzylic) = 45.3, $4a_H$(methylene) = 45.0, $4a_H$(ortho) = 13.9, $4a_H$(meta) = 4.84, and $2a_H$(para) = 17.2 MHz; g (same for each radical center) = 2.0026. Three spin relaxation rates were included: two correlated dipolar rates (k_{d1} and k_{d2}, single and double spin flips, respectively) and one uncorrelated dipolar rate (k_u). Specifically for **1b**: $J = (-9.5 \pm 0.3) \times 10^3$ MHz, $k_{en} = (6.0 \pm 0.5) \times 10^9\ s^{-1}$. At X-band (spectrum A): initial populations of $T^+:T^0:T^-$ = 0.321:0.321:0.358, $k_{d1} = k_{d2} = 1 \times 10^5\ s^{-1}$, $k_u = 2 \times 10^6\ s^{-1}$, line width (LW) = 2.0 G. At Q-band (spectrum B): initial populations of $T^+:T^0:T^-$ = 0.323:0.323:0.353, $k_{d1} = k_{d2} = 5 \times 10^6\ s^{-1}$, $k_u = 2.8 \times 10^7\ s^{-1}$, LW = 10 G. Specifically for **1a**: $J = -2 \times 10^4$ MHz (lower limit), $k_{en} = 1.2 \times 10^{10}\ s^{-1}$ (lower limit). At X-band (spectrum C): $k_{d1} = k_{d2} = 3 \times 10^6\ s^{-1}$, $k_u = 5 \times 10^6\ s^{-1}$, LW = 5 G. At Q-band (spectrum D): $k_{d1} = k_{d2} = 1 \times 10^6\ s^{-1}$, $k_u = 5 \times 10^6\ s^{-1}$, LW = 3 G. Initial populations of $T^+:T^0:T^-$ = 0.333:0.333:0.333 were used at both X-band and Q-band for **1a**.

Our experimental method has been described previously for X-band,[7] and a detailed description of our Q-band spectrometer is the subject of a recent publication.[8] Figure 2 shows experimental results and simulations for biradicals **1a** and **1b** at both frequencies. The overall emissive polarization observed for the two chain lengths at Q-band confirms a negative value for $2J$ (singlet ground state), in accordance with theoretical predictions.[9] The absorptive polarization in the X-band spectrum of **1b** is due to the triplet mechanism[10] and is accounted for in the simulation. In fact, the spectrum of **1b** is also absorptive at early times at Q-band but becomes emissive more quickly than at X-band. This is predicted from theory for a biradical with a large negative value of $2J$. The spectrum from **1a** was emissive at both frequencies at even the earliest detectable delay times (~50 ns) after the flash.

For both chain lengths the signal intensities at Q-band were much stronger than at X-band, indicating that the correlated radical pair (CRP) spin polarization observed is field-dependent and that $|2J|$ is larger than the X-band Zeeman energy. Since the overall sensitivity of the Q-band bridge is quite poor,[11] the polarization enhancement in the high-frequency spectra must be very large. The spectrum of **1a** at X-band was just barely observable 100 ns after the laser flash and could not be observed at any later delay times. The J coupling of **1a** was found to be larger than that for **1b**, and its spectrum is somewhat featureless. However, it can be safely assigned on the basis of the following observations: (1) the totally emissive polarization is correct for a ground-state singlet biradical with a large singlet–triplet energy gap originating from a triplet precursor, (2) the EPR signal lifetime compares favorably to that measured optically by Turro and co-workers at 0 magnetic field,[12,13] (3) the spectral width of the simulation matches experiment using the same hyperfine coupling constants as for **1b**, and (4) there is a significant increase in the magnitude of the polarization enhancement for **1a** at higher applied fields.

---

(6) (a) Delocalized 1,5- and 1,7-biradicals have been observed by fluorescence excitation in low-temperature matrices and by laser flash photolysis in solution: Biewer, M. C.; Biehn, C. R.; Platz, M. S.; Després, A.; Migirdicyan, E. *J. Am. Chem. Soc.* **1991**, *113*, 616. (b) Recently, we observed radical pair mechanism CIDEP in doublet-state radicals and magnetic field effects in longer biradicals at Q-band: Forbes, M. D. E. *J. Phys. Chem.* **1992**, *96*, 7836.

(7) (a) Forbes, M. D. E.; Dukes, K. E.; Myers, T. L.; Maynard, H. D.; Breivogel, C. S.; Jaspan, H. B. *J. Phys. Chem.* **1991**, *95*, 10547. (b) Forbes, M. D. E.; Peterson, J.; Breivogel, C. S. *Rev. Sci. Instrum.* **1991**, *62*, 2662.

(8) Forbes, M. D. E. *Rev. Sci. Instrum.* **1993**, *64*, 397.

(9) Dougherty, D. A.; Goldberg, A. H. *J. Am. Chem. Soc.* **1983**, *105*, 284.

(10) (a) *Spin Polarization and Magnetic Effects in Radical Reactions*; Molin, Yu. N., Ed.; Elsevier: New York, 1984; pp 224–242. (b) Atkins, P. W.; Evans, G. T. *Mol. Phys.* **1974**, *27*, 1633.

(11) Hyde, J. S.; Newton, M. E.; Strangeway, R. A.; Camenisch, T. G.; Froncisz, W. *Rev. Sci. Instrum.* **1991**, *62*, 2969.

(12) Zimmt, M. B.; Doubleday, C., Jr.; Turro, N. J. *Chem. Phys. Lett.* **1987**, *134*, 549.

(13) The overall signal intensity of **1a** decayed over approximately 1 μs, and that of **1b** over 1.5 μs. These lifetimes are slightly longer than measured by Zimmt et al. in ref 12, which is the expected result when the energies of the triplet levels are split by an applied magnetic field.

The simulations were run using a computer program based on a model described previously,[4b] using parameters listed in the caption of Figure 2. The *J* couplings are smaller than those for bis(alkyl) biradicals of even longer chain length,[4] indicating that delocalizing the electrons into the aromatic rings results in a significant decrease in the interaction between them, as expected. An analysis of the time evolution of all four EPR signals, especially with regard to spin relaxation and chemical reaction rates, is the subject of research in progress. From these preliminary simulations, we can conclude that both correlated and uncorrelated electron dipole–dipole induced spin relaxation plays a strong role in determining the shape of the spectra. Spin–orbit coupling appears to manifest itself only in the overall disappearance of the signals on the microsecond time scale.

Acknowledgment. The author thanks the National Science Foundation for support of this research through Grant CHE-9200917.

---

(14) Dana, D. E.; Hay, A. S. *Synthesis* **1982**, 164.

(15) *Landolt-Bornstein New Series, Group II*; Springer–Verlag: New York, 1979; Vol. 9b.

(16) (a) Forbes, M. D. E., unpublished results. (b) Koptyug, I., private communication.

Solution Structure of an Intramolecular Purine·Purine·Pyrimidine DNA Triplex

Ishwar Radhakrishnan[†] and Dinshaw J. Patel*[,†,‡]

Department of Biochemistry and Molecular Biophysics
College of Physicians and Surgeons, Columbia University
New York, New York, 10032
Program in Cellular Biochemistry and Biophysics
Rockefeller Research Laboratories
Memorial Sloan-Kettering Cancer Center
New York, New York 10021

Received November 16, 1992

The sequence-specific recognition of DNA duplexes by third strands through triplex formation[1] has potential applications ranging from gene regulation[2] to site-specific cleavage of genomic DNA.[3] This effort could be greatly aided by a knowledge of the structural details of DNA triplexes in solution and in the crystalline state. There has been no success in the latter approach to date, and we report below on continued progress in defining the solution structure of DNA triplexes through a combination of NMR experiments and molecular dynamics computations.

The pyrimidine·purine·pyrimidine (Y·RY) DNA triplex has the third pyrimidine strand positioned in the major groove and *parallel* to the purine strand of the Watson–Crick duplex.[4] Several Y·RY triplexes containing standard T·AT and C^+·GC triples as well as other triplex combinations have been investigated in solution by NMR.[5] We have recently determined the solution structure of a G·TA-containing Y·RY triplex by a combination of experimental NMR constraints and molecular dynamics calculations,[6] in contrast to Y·RY triplex models based on computations alone.[7] The purine·purine·pyrimidine (R·RY) DNA triplex has the third purine-rich strand positioned in the major groove *antiparallel* to the purine strand of the Watson–Crick duplex.[8] This triplex is stabilized by G·GC[8c,8d] and A/T·AT[8d] triples (supplementary Figure 1), and solution NMR studies have established that the third strand bases adopt *anti* glycosidic torsion angles,[9] thus defining the base triple pairing alignments. We report below on a combined NMR–molecular dynamics study which defines the solution structure of an intramolecular R·RY triplex (**1**) and identifies the structural transitions necessary for accommodating thymines in an otherwise guanine-rich third strand.

Figure 1. (A) Best fit superposition of the six refined structures. (B) Representative refined structure of the G17-T18-G19-G20 segment of the purine-rich third strand of the R·RY triplex **1**. Note the increase in helical rise between T18 and G19 at the T-G step.

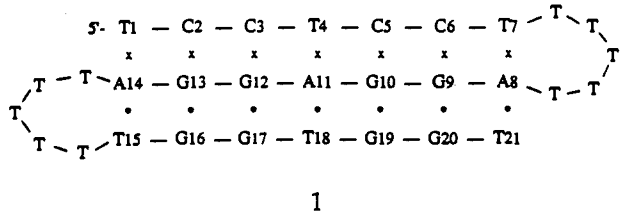

1

The intramolecular[10] R·RY triplex **1**, which contains two partially overlapping T-G-G-T repeats in the third strand, was chosen since it gave narrower exchangeable and nonexchangeable proton spectra (supplementary Figures 2A and 2B) than its

---

[†] Columbia University.

[‡] Memorial Sloan-Kettering Cancer Center.

(1) (a) Felsenfeld, G.; Davies, D.; Rich, A. *J. Am. Chem. Soc.* **1957**, *79*, 2023–2024. (b) Lee, J. S.; Johnson, D. A.; Morgan, A. R. *Nucl. Acids Res.* **1979**, *6*, 3073–3091. (c) Arnott, S.; Bond, P. J.; Selsing, E.; Smith, P. J. C. *Nucl. Acids Res.* **1976**, *3*, 2459–2470. (d) Reviewed: Wells, R. D.; Collier, D. A.; Hanvy, J. C.; Shimuzu, M.; Wohlraub, F. *FASEB J.* **1988**, *2*, 2939–2949.

(2) (a) Postel, E. H.; Flint, S. J.; Kessler, D. J.; Hogan, M. E. *Proc. Natl. Acad. Sci. U.S.A.* **1991**, *88*, 8227–8231. (b) Maher, L. J.; Dervan, P. B.; Wold, B. *Biochemistry* **1992**, *31*, 70–81. (c) Duval-Valentin, G.; Thuong, N. T.; Helene, C. *Proc. Natl. Acad. Sci. U.S.A.* **1992**, *89*, 504–508.

(3) (a) Strobel, S. A.; Dervan, P. B. *Science* **1990**, *249*, 73–75. (b) Strobel, S. A.; Dervan, P. B. *Nature* **1991**, *350*, 172–174.

(4) (a) Moser, H.; Dervan, P. B. *Science* **1987**, *238*, 645–650. (b) Le Doan, T.; Perronault, L.; Praseuth, D.; Habhoub, N.; Decout, J. L.; Thuong, N. T.; Lhomme, J.; Helene, C. *Nucl. Acids Res.* **1987**, *15*, 7749–7760. (c) Hanvey, J. C.; Shimuzu, M.; Wells, R. D. *Proc. Natl. Acad. Sci. U.S.A.* **1988**, *85*, 6292–6296. (d) Plum, G. E.; Park, Y. W.; Singleton, S. F.; Dervan, P. B.; Breslauer, K. J. *Proc. Natl. Acad. Sci. U.S.A.* **1990**, *87*, 9436–9440. (e) Roberts, R. W.; Crothers, D. M. *Proc. Natl. Acad. Sci. U.S.A.* **1991**, *88*, 9397–9401. (f) Yoon, K.; Hobbs, C. A.; Koch, J.; Sardaro, M.; Kutny, R.; Weis, A. L. *Proc. Natl. Acad. Sci. U.S.A.* **1992**, *89*, 3840–3844.

(5) (a) De los Santos, C.; Rosen, M.; Patel, D. J. *Biochemistry* **1989**, *28*, 7282–7288. (b) Rajagopal, P.; Feigon, J. *Biochemistry* **1989**, *28*, 7859–7870. (c) Mooren, M. M.; Pulleyblank, D. E.; Wizmenga, S. S.; Bloomers, M. J.; Hilbers, C. W. *Nucl. Acids Res.* **1990**, *18*, 6523–6529. (d) Radhakrishnan, I.; Gao, X.; De los Santos, C.; Live, D.; Patel, D. J. *Biochemistry* **1991**, *30*, 9022–9030. (e) Macaya, R. F.; Gilbert, D. E.; Malek, S.; Sinsheimer, J. S.; Feigon, J. *Science* **1991**, *254*, 270–274. (f) Radhakrishnan, I.; Patel, D. J.; Gao, X. *Biochemistry* **1992**, *31*, 2514–2523. (g) Macaya, R. F.; Wang, F.; Schultze, P.; Sklenar, V.; Feigon, J. *J. Mol. Biol.* **1992**, *225*, 755–773. (h) Wang, E.; Malek, S.; Feigon, J. *Biochemistry* **1992**, *31*, 4838–4846.

(6) Radhakrishnan, I.; Patel, D. J.; Veal, J. M.; Gao, X. *J. Am. Chem. Soc.* **1992**, *114*, 6913–6915.

(7) Laughton, C. A.; Neidle, S. *J. Mol. Biol.* **1992**, *223*, 519–529.

(8) (a) Cooney, M.; Czernuszewicz, G.; Postel, E. H.; Flint, S. J.; Hogan, M. E. *Science* **1988**, *241*, 456–459. (b) Letai, A. G.; Palladino, M. A.; Fromm, E.; Rizzo, V.; Fresco, J. R. *Biochemistry* **1988**, *27*, 9108–9112. (c) Kohwi, Y.; Kohwi-Shigematsu, T. *Proc. Natl. Acad. Sci. U.S.A.* **1988**, *85*, 3781–3785. (d) Beal, P. A.; Dervan, P. B. *Science* **1991**, *251*, 1360–1363. (e) Durland, R. H.; Kessler, D. J.; Gunnell, S.; Duvie, M.; Pettitt, B. M.; Hogan, M. E. *Biochemistry* **1991**, *30*, 9246–9255. (f) Pilch, D. S.; Levenson, C.; Shafer, R. H. *Biochemistry* **1991**, *30*, 6081–6087. (g) Sun, J.; De Bizemont, T.; Duval-Valentin, G.; Montenay-Garestier, T.; Helene, C. *C. R. Acad. Sci. Paris* **1991**, *313*, 585–590. (h) Chen, F. M. *Biochemistry* **1991**, *30*, 4472–4479. (i) Durland, R. H.; Kessler, D. J.; Gunnell, S.; Duvic, M.; Pettitt, B. M.; Hogan, M. E. *Biochemistry* **1991**, *30*, 9246–9255. (j) Beal, P. A.; Dervan, P. B. *Nucl. Acids Res.* **1992**, *20*, 2773–2776.

(9) Radhakrishnan, I.; De los Santos, C.; Patel, D. J. *J. Mol. Biol.* **1991**, *221*, 1403–1418.

(10) (a) Haner, R.; Dervan, P. B. *Biochemistry* **1990**, *29*, 9761–9765. (b) Sklenar, V.; Feigon, J. *Nature* **1990**, *345*, 836–838. (c) Radhakrishnan, I.; Patel, D. J.; Gao, X. *J. Am. Chem. Soc.* **1991**, *113*, 8542–8544.

0002-7863/93/1515-1615$04.00/0